

Expansion of a coherent array of Bose-Einstein condensates

P. Pedri, L. Pitaevskii*, S. Stringari

Dipartimento di Fisica, Università di Trento and Istituto Nazionale per la Fisica della Materia, I-38050 Povo, Italy
**Kapitza Institute for Physical Problems, Moscow, Russia*

C. Fort, S. Burger, F. S. Cataliotti, P. Maddaloni, F. Minardi, M. Inguscio

*LENS, Dipartimento di Fisica, Università di Firenze and Istituto Nazionale per la Fisica della Materia, L.go E. Fermi 2,
I-50125 Firenze, Italy*
(July 7, 2021)

We investigate the properties of a coherent array containing about 200 Bose-Einstein condensates produced in a far detuned 1D optical lattice. The density profile of the gas, imaged after releasing the trap, provides information about the coherence of the ground-state wavefunction. The measured atomic distribution is characterized by interference peaks. The time evolution of the peaks, their relative population as well as the radial size of the expanding cloud are in good agreement with the predictions of theory. The 2D nature of the trapped condensates and the conditions required to observe the effects of coherence are also discussed.

PACS numbers: 03.75.Fi, 32.80.Pj

Coherence is one of the most challenging features exhibited by Bose-Einstein condensates. On the one hand it underlies the superfluid phenomena exhibited by these cold atomic gases. On the other hand it characterizes in a unique way their matter wave nature at a macroscopic level. Coherence requires that the system be characterized by a well defined phase, giving rise to interference phenomena.

After the first interference measurements carried out on two expanding condensates at MIT [1] the experimental study of interference in Bose-Einstein condensed gases has become an important activity of research opening the new field of coherent atom-optics.

The possibility of confining Bose-Einstein condensates in optical lattices has opened further perspectives in the field [2]. Bose-Einstein condensates confined in an optical standing-wave provide in fact a unique tool to test at a fundamental level the quantum properties of systems in periodic potentials. The observation of interference patterns produced by an array of condensates trapped in an optical lattice was already used as a probe of the phase properties of this system [3,4] also allowing to proof the phase relation in an oscillating Josephson current [5]. In [3] the interference effect has been used to explore the emergence of number squeezed configurations in optically trapped condensates.

The main purpose of this paper is to investigate the ground state properties of the system of a fully coherent array of condensates. To this aim we have explored the interference pattern in the expanded cloud, reflecting the initial geometry of the sample.

The basic phenomenon we want to explore is the atom optical analog of light diffraction from a grating. The analogy is best understood considering a periodic and coherent array of identical condensates aligned along the x -axis. In momentum space the order parameter takes the form

$$\begin{aligned}\Psi(p_x) &= \Psi_0(p_x) \sum_{k=0, \pm 1, \dots, \pm k_M} e^{\frac{ik_p d}{\hbar}} \\ &= \Psi_0(p_x) \frac{\sin[(2k_M + 1)p_x d / 2\hbar]}{\sin p_x d / 2\hbar}\end{aligned}\quad (1)$$

where k labels the different sites of the lattice, $2k_M + 1$ is the total number of sites (in the following we will assume $k_M \gg 1$) and d is the distance between two consecutive condensates. The quantity $n_0(p_x) = |\Psi_0(p_x)|^2$ is the momentum distribution of each condensate (see Eq. (5) below). The momentum distribution of the whole system, given by $n(p_x) = |\Psi(p_x)|^2$, is affected in a profound way by the lattice structure and exhibits distinctive interference phenomena. Actually the effects of coherence are even more dramatic than in the case of two separated condensates [6]. Indeed, in the presence of the lattice the momentum distribution is characterized by sharp peaks at the values $p_x = n2\pi\hbar/d$ with n integer (positive or negative) whose weight is modulated by the function $n_0(p_x)$. Furthermore, differently from the case of two separated condensates, interference fringes appear only if the initial configuration is coherent. In principle the momentum distribution can be directly measured *in situ* using 2-photon Bragg spectroscopy. This possibility has been already implemented experimentally for a single condensate [7]. However, the very peculiar structure of (1) is expected to influence in a deep way also the expansion of the atomic cloud after the release of the trap. The width of the central peak ($n = 0$) of the momentum distribution is of the order $\Delta p_x \sim \hbar/R_x$ where $R_x \sim k_M d$ is half of the length of the whole sample in the x -direction and the corresponding atomic motion, after the release of the trap, will be consequently slow. On the other hand the peaks with $n \neq 0$ carry high momentum and the center of mass of these peaks will expand fast according to the asymptotic law

$$x(t) = \pm n \frac{2\pi\hbar}{dm} t. \quad (2)$$

The occurrence of these peaks is the analog of multiple order interference fringes in light diffraction.

We create an array of BECs of ^{87}Rb in the $|F = 1, m_F = -1\rangle$ state by superimposing the periodic optical potential V_{opt} of a far detuned standing-wave on the harmonic potential V_B of the magnetic trap. For a more detailed description see [8,9]. The resulting potential is given by

$$V = V_B + V_{opt} = \frac{1}{2}m(\omega_x^2 x^2 + \omega_\perp^2(y^2 + z^2)) + sE_R \cos^2(qx + \frac{\pi}{2}) \quad (3)$$

with m the atomic mass, $\omega_x = 2\pi \times 9$ Hz and $\omega_\perp = 2\pi \times 92$ Hz the axial and radial frequency of the magnetic harmonic potential and x lying in the horizontal plane. In (3) s is a dimensionless factor, $q = 2\pi/\lambda$ is the wavevector of the laser light creating the standing wave and producing local minima in V_{opt} separated by $d = \lambda/2$ and $E_R = \hbar^2 q^2 / 2m \sim 2\pi\hbar \times 3.6$ kHz is the recoil energy of an atom absorbing one lattice photon. By varying the intensity of the laser beam (detuned 150 GHz to the blue of the D_1 transition at $\lambda = 795$ nm) up to 14 mW/mm² we can vary the intensity factor s from 0 to 5. We calibrated the optical potential measuring the Rabi frequency (Ω_R) of the Bragg transition between the momentum states $-\hbar q$ and $+\hbar q$ induced by the standing wave. The intensity factor is then given by $s = 2\hbar\Omega_R/E_R$ [10].

The procedure to load the condensate in the combined (magnetic+optical) trap is the following: we load ^{87}Rb atoms in the magnetic trap and cool the sample via rf-forced evaporation until a significant fraction of condensed atoms is produced. We then switch on the laser standing-wave and continue the evaporative cooling to a lower temperature ($T \ll T_c$). Typically, the BEC splits over ~ 200 wells, each containing $100 \sim 500$ atoms. After switching off the combined potential we let the system expand and take an absorption image of the cloud at different expansion times t_{exp} .

In Fig. 1A we show a typical image of the cloud taken at $t_{exp} = 29.5$ ms, corresponding to a total number of atoms $N = 20000$ and to a laser intensity $s = 5$. From the images taken after the expansion we can determine the relative population of the lateral peak with respect to the central one. The experimental results for the relative population of the first lateral peak as a function of the laser intensity s are shown in Fig. 2.

The structure of the observed density profiles is well reproduced by the free expansion of the ideal gas where the time evolution of the order parameter, in coordinate space, takes the form:

$$\Psi(x, t) = \frac{1}{(2\pi)^3} \int dp_x \Psi(p_x) e^{ip_x x/\hbar} e^{-ip_x^2 t/2m\hbar} \quad (4)$$

For a realistic description of $\Psi(p_x)$ we have improved the simple ansatz (1) in order to account for the k -dependence of the number of atoms N_k contained in

each well. Due to magnetic trapping, the central condensates with $k \ll k_M$ will be in fact more populated than the ones occupying the sites at the periphery. We have accounted for the modulation by the simple law $N_k = N_0(1 - k^2/k_M^2)^2$ which will be derived below. For Ψ_0 we have made the Gaussian choice

$$\Psi_0(p_x) \propto \exp[-p_x^2 \sigma^2 / 2\hbar^2] \quad (5)$$

corresponding, in coordinate space, to $\Psi_0(x) \sim \exp[-x^2/2\sigma^2]$. Using (5) it is immediate to find that the relative population of the $n \neq 0$ peaks with respect to the central one ($n = 0$) obeys the simple law

$$P_n = \exp[-4\pi^2 n^2 \sigma^2 / d^2] \quad (6)$$

holding also in the presence of a smooth modulation of the atomic occupation number N_k in each well. Result (6) shows that, if σ is much smaller than d the intensity of the lateral peaks will be high, with a consequent important layered structure in the density distribution of the expanding cloud. The value of σ , which characterizes the width of the condensates in each well, is determined, in first approximation, by the optical confinement. The simplest estimate is obtained by the harmonic expansion of the optical potential (3) around its minima: $V = \sum_k (1/2)m\tilde{\omega}_x^2(x - kd)^2$ with $\tilde{\omega}_x = 2\sqrt{s}E_R/\hbar$, yielding $\sigma = d/(\pi s^{1/4})$. However this estimate is not accurate except for very intense laser fields. A better value is obtained by numerical minimization of the energy using the potential (3) and the wavefunction (5). This gives $\sigma/d = 0.30, 0.27,$ and 0.25 for $s = 3, 4$ and 5 respectively. The predicted results for the density distribution $n(x) = |\Psi(x)|^2$ evaluated for $s = 5$ and $t = 29.5$ ms are shown in Fig. 1B (continuous line).

From the above calculation we can also determine the relative population P_n of the $n = 1$ peak as a function of the intensity factor s . This is shown in Fig. 2 together with the experimental results. The good comparison between experiment and theory reveals that the main features of the observed interference patterns are well described by this simple model.

The 1D model discussed above can be generalized to 3D through the ansatz

$$\Psi_0(\mathbf{r}) = \sum_{k=0, \pm 1, \dots, \pm k_M} e^{-(x-kd)^2/2\sigma^2} \Psi_k(\mathbf{r}_\perp) \quad (7)$$

which can be used, through a variational calculation, to describe the ground state of the system in the presence of the optical potential, magnetic trapping and two-body interactions. For sufficiently intense optical fields the value of σ is not significantly affected by two-body interactions, nor by magnetic trapping. On the other hand interactions are important to fix the shape of the condensate wave function in the radial direction. Neglecting the small overlap between condensates occupying different sites and using the Thomas-Fermi approximation to

determine the wave function in the radial direction we obtain the result

$$|\Psi_k(\mathbf{r}_\perp)|^2 = \frac{\sqrt{2}}{g} \mu_k \left(1 - \frac{r_\perp^2}{(R_\perp)_k^2} \right) \quad (8)$$

where $(R_\perp)_k = \sqrt{2\mu_k/m\omega_\perp^2}$ is the radial size of the k -th condensate, g depends on the scattering length a through the relation $g = 4\pi\hbar^2 a/m$, while

$$\mu_k = \frac{1}{2} m \omega_x^2 d^2 (k_M^2 - k^2) \quad (9)$$

plays the role of an effective k -dependent chemical potential. The value of k_M is fixed by the normalization condition $N = \sum N_k$ and is given by

$$k_M^2 = \frac{2\hbar\bar{\omega}}{m\omega_x^2 d^2} \left(\frac{15}{8\sqrt{\pi}} N \frac{a}{a_{ho}} \frac{d}{\sigma} \right)^{2/5}. \quad (10)$$

In (10) $\bar{\omega} = (\omega_x \omega_\perp^2)^{1/3}$ is the geometrical average of the magnetic frequencies, $a_{ho} = \sqrt{\hbar/m\bar{\omega}}$ is the corresponding oscillator length and a is the s -wave scattering length. From the above equations one also obtains the result $N_k = N_0(1 - k^2/k_M^2)^2$ with $N_0 = (15/16)N/k_M$. Equations (8-10) generalize the well known Thomas-Fermi results holding for magnetically trapped condensates [11] to include the effects of the optical lattice.

Neglecting two-body interaction terms in the determination of the Gaussian width in the x -direction is a good approximation only if μ_k is significantly smaller than the energy $\hbar\tilde{\omega}_x$. This condition is rather well satisfied in the configurations of higher lattice potential employed in the experiment. For example, using the typical parameter $N = 5 \times 10^4$ for the total number of atoms and the values $\bar{\omega} = 2\pi \times 42$ Hz and $a/a_{ho} = 3.2 \times 10^{-3}$, we find, for $s = 4$, $\tilde{\omega}_x \sim 2\pi \times 14$ kHz, $\mu_{k=0} \sim 2\pi\hbar \times 0.5$ kHz and $k_M \sim 100$, corresponding to $N_0 \sim 500$. Notice that with these values the condition $\mu_k \gg \hbar\omega_\perp$ required to apply the Thomas-Fermi approximation is rather well satisfied for the central wells.

The fact that μ_k turns out to be significantly smaller than $\hbar\tilde{\omega}_x$ not only explains why the interference patterns emerging during the expansion are well described by the ideal 1D model for the array used above, but also points out the 2D nature of the condensates confined in each well. In this context it is worth pointing out that the bidimensionality of these condensates is ensured up to temperatures of the order of $k_B T \sim \hbar\tilde{\omega}_x$, which is significantly higher than the expected value of the critical temperature for Bose-Einstein condensation. Our sample can then be used also to explore the consequence of the array geometry on the critical phenomena exhibited by these optically trapped Bose gases [12].

The above discussion permits also to explain the behaviour of the radial expansion of the gas. In the presence of the density oscillations produced by the optical lattice the problem is not trivial and should be solved

numerically by integrating the GP equation. However, after the lateral peaks are formed, the density of the central peak expand smoothly according to the asymptotic law $R_\perp(t) = R_\perp(0)\omega_\perp t_{exp}$, holding for a cigar configuration in the absence of the optical lattice [13]. In Fig. 3 the linear law is plotted using the expression $R_\perp(0) \sim (R_\perp)_{k=0} = k_M d \omega_x / \omega_\perp$ derivable from Eq. (9) for the condensate occupying the central well. This choice for $R_\perp(0)$ is justified if the population of the lateral interference peaks is small so that their creation does not affect the radial expansion of the system.

Let us finally discuss the conditions required for our system to exhibit coherence. At zero temperature the coherence between two consecutive condensates in the array is ensured if $E_c \ll E_J$, where E_c and E_J are the parameters of the Josephson Hamiltonian for two adjacent condensates [14]. In particular $E_c = 2\partial\mu_k/\partial N_k$ is the interaction parameter while $E_J = (\hbar^2/m) \int d\mathbf{r}_\perp [\Psi_k \partial \Psi_{k+1} / \partial x - \Psi_{k+1} \partial \Psi_k / \partial x]_{x=0}$ is the Josephson parameter describing the tunneling rate through the barrier separating two consecutive wells. In our case ($s = 4$ and $N = 5 \times 10^4$) we find $E_c \sim 2\pi\hbar \times 1$ Hz for the most relevant central condensates ($k \ll k_M$) while, by solving numerically the Schrödinger equation in the presence of the optical potential V_{opt} of Eq. (3), we find $E_J \sim 2\pi\hbar \times 600$ kHz. The value of E_J is so large that one can safely conclude that the ground state of the system is fully coherent and that the effects of the quantum fluctuations of the phase will be consequently negligible. This reflects the fact that, even for the largest values employed for the laser power the overlap between consecutive condensates is not small enough. The value of E_J is also much higher than the values of $k_B T$ used in the experiment, so that also the effects of the thermal fluctuations of the phase of the condensate can be ignored. This suggests that the fringes associated with the expansion of the condensate will remain visible up to the highest values of T , corresponding to the critical temperature for Bose-Einstein condensation. We have carried out experiments at different values of T where the signal obtained by imaging the expanding cloud can be naturally decomposed in two parts: an incoherent component due to the thermal cloud which is parametrized by a classical Gaussian Boltzmann distribution, and a Bose-Einstein component exhibiting the interference effects discussed above. In our experiment the interference peaks are visible up to $k_B T \sim 2\pi\hbar \times 4.2$ kHz. In order to point out the effects of the fluctuations of the phase one should lower the value of E_J by orders of magnitude. This can be achieved by increasing significantly the laser power generating the optical lattice. Such effects have been recently observed in the experiment of [3].

In conclusion, we have investigated the consequences of coherence on the properties of an array of Bose-Einstein condensates. We have observed peculiar interference patterns in the density of the expanded cloud, reflecting the new geometry of the sample and discussed on a theoretical basis some key features exhibited by these optically

trapped gases. Further studies in this direction include the possible effects of thermal decoherence [15,16] in the presence of tighter optical traps and the emergence of $2D$ effects in the thermodynamic properties of these novel systems.

This work has been supported by the EU under Contracts No. HPRI-CT 1999-00111 and No. HPRN-CT-2000-00125, by the MURST through the PRIN 1999 and PRIN 2000 Initiatives and by the INFN Progetto di Ricerca Avanzata "Photon matter".

-
- [1] M. R. Andrews *et al.*, Science **275**, 637 (1997).
 - [2] B. P. Anderson and M. A. Kasevich, Science **282**, 1686 (1998).
 - [3] C. Orzel *et al.*, Science **291**, 2386 (2001).
 - [4] M. Greiner *et al.*, cond-mat/0105105.
 - [5] F. S. Cataliotti *et al.*, Science accepted for publication.
 - [6] L. Pitaevskii and S. Stringari, Phys. Rev. Lett. **83**, 4237 (1999).
 - [7] D. M. Stamper-Kurn *et al.*, Phys. Rev. Lett. **83**, 2876 (1999).
 - [8] C. Fort *et al.*, Europhys. Lett. **49**, 8 (2000).
 - [9] S. Burger *et al.*, Phys. Rev. Lett. **86**, 4447 (2001).
 - [10] E. Peik *et al.*, Phys. Rev. A **55**, 2989 (1997).
 - [11] F. Dalfovo, S. Giorgini, L. P. Pitaevskii, and S. Stringari, Rev. Mod. Phys. **71**, 463 (1999).
 - [12] S. Burger *et al.* in preparation.
 - [13] Y. Castin and R. Dum, Phys. Rev. Lett. **77**, 5315 (1996).
 - [14] A. J. Leggett, Rev. Mod. Phys. **73**, 307 (2001).
 - [15] L. Pitaevskii and S. Stringari, cond-mat/0104458.
 - [16] A. Cuccoli, A. Fubini, V. Tognetti, and R. Vaia, cond-mat/0107387

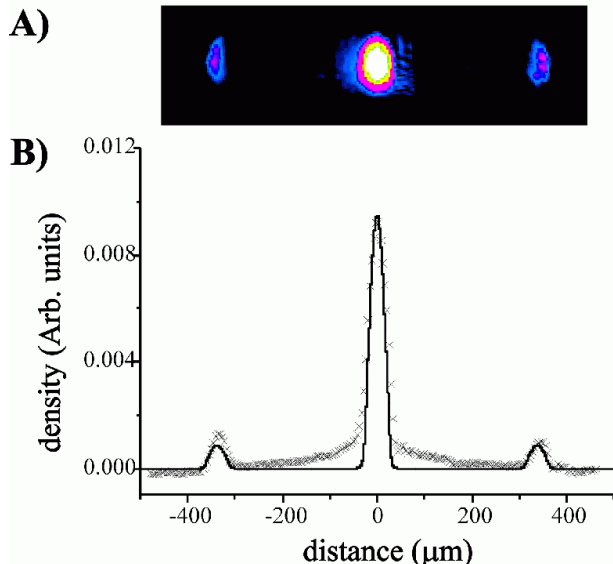


FIG. 1. A) Absorption image of the density distribution of the expanded array of condensates. B) Experimental density profile (crosses) obtained from the absorption image (A) integrated along the vertical direction. The wings of the central peak result from a small thermal component. The continuous line corresponds to the calculated density profile for the expanded array of condensates for the experimental parameters ($s = 5$ and $t_{exp} = 29.5$ ms).

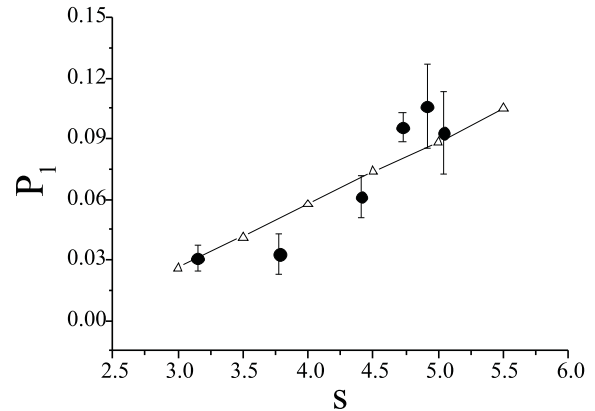


FIG. 2. Experimental (circles) and theoretical (triangles) values of the relative population of the $n = 1$ peak with respect to the $n = 0$ central one as a function of the intensity factor s of the optical potential V_{opt} .

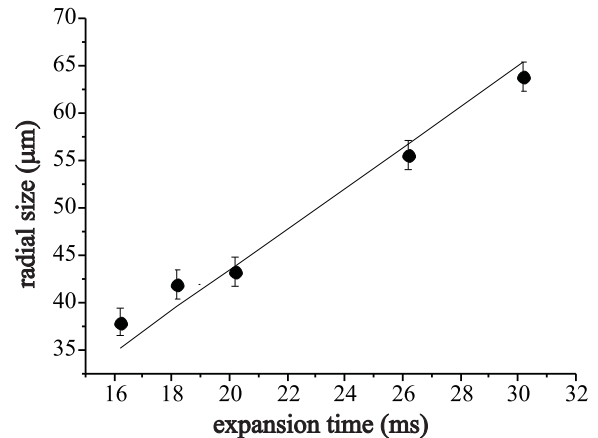


FIG. 3. Radial size of the central peak as a function of the expansion time. Experimental data point are compared with the expected asymptotic law $R_{\perp} = R_{\perp}(0)\omega_{\perp}t_{exp}$.